TEMPERATURE RISE CHARACTERISTICS OF SINGLE LITHIUM IRON PHOSPHATE BATTERY

Xinguang LI*[1], Jiayu YUAN[1], Wenchao WANG[1]

In order to explore the influence of the structural parameters of square single lithium iron phosphate battery on the temperature rise law of electric vehicle, the NTGP Table model is used to construct a three-dimensional electrochemical-thermal coupling model of the single lithium battery. The temperature rise test of single lithium battery 1C and 2C discharge rate under normal temperature conditions is carried out, and the temperature rise law of single lithium battery is obtained. The accuracy of the three-dimensional electrochemical-thermal coupling model is verified by experimental data. Furthermore, a simulation study on the temperature distribution of single cells with different thicknesses and conductivity coefficients of bipolar plate is carried out. The simulation results show that the temperature distribution of the single lithium battery is uneven, and the highest temperature occurs near the positive tab, followed by the negative tab. The greater the thickness of the current collector, the smaller the maximum temperature rise, and the highest temperature at the positive electrode of the battery. As the conductivity increases, its effect on the maximum temperature of battery discharge decreases gradually.

Keywords: Lithium iron phosphate power battery; temperature rise test; temperature field; bipolar plate; conductivity

1. Introduction

As the energy source of electric vehicles, the working performance of the power battery pack is greatly affected by the ambient temperature. If the cooling system of the battery fails to reach the predetermined heat dissipation for a long time, it will lead to the decline of battery performance, reduce its service life, and even cause safety accidents such as battery combustion and explosion [1-3]. The thermal effects of lithium batteries have been researched extensively. Armando et al. [4] presents a computational modeling approach to characterize the internal temperature distribution within a Li-Ion battery pack. The model is then used to simulate air-cooling and a liquid-cooling strategies for the thermal control of a battery pack in case of car application. Karthik et al. [5] obtains optimal mass flow rate combination of coolant in the channels for reducing the power consumption of the battery thermal management systems by using multi-objective optimization technique coupled with computational fluid dynamics simulations. Akbarzadeh et al. [6] conducted a comparative analysis between air type and liquid type thermal

[1] School of Mechanical &Automotive Engineering Qingdao University of Technology, Qingdao266500, China
* Corresponding author: e-mail: tutulxg@126.com

management systems for a high-energy lithium-ion battery module.

Zhang et al. [7] established a three-dimensional model to study the temperature rise characteristics of batteries in discharge. Li et al. [8] explored the battery voltage and temperature changes under different discharge rates by constructing a three-dimensional electrochemical-thermal model. Wang et al.[9] simulated the temperature distribution of the single battery and the location of the highest temperature of the battery. Zhu et al. [10] applied the three-dimensional thermoelectric coupling model to analyze the effects of end collector structure, cell size and heat dissipation mode on the battery temperature. The three-dimensional battery model established by Yang et al. [11] considered the thermal characteristics of battery materials and verified the accuracy of the model through battery testing. Kuang et al. [12] established a two-dimensional battery simulation model and simulate the batteries with 10-150 cm electrodes of lengths. Sheng et al. [13] considered the boundary conditions of natural convection and thermal radiation to simulate the temperature rise characteristics of the battery cells. Veth et al. [14] studied and analyzed the highest and lowest temperature points and temperature gradients in large-capacity lithium-ion soft-pack batteries.

The above electrochemical-thermal coupling simulations of the single battery mostly use the simplified Bernardi heat generation theory to calculate the battery heat generation rate [15]. The battery discharge is a dynamic process. As the SOC (State of Charge) changes, the discharge voltage gradually decreases, and the heat generation rate also changes accordingly. Therefore, this paper adds the battery SOC model to the Bernardi heat generation model to improve the accuracy of battery thermal simulation. Meanwhile, different physical and chemical parameters of battery materials will affect the internal resistance and heat transfer of the battery. In this paper, based on the NTGP Table (Newman Tiedemann Gu Peukert) model, the temperature rise characteristics of single prismatic lithium batteries under different current collector thicknesses and conductivity coefficients are simulated.

2. Temperature rise characteristic test of single prismatic lithium battery

In order to obtain the temperature rise law of the single prismatic lithium battery when discharged at 1C and 2C rates, the temperature rise of the single battery was subjected to a discharge test at 25°C.

2.1 Construction of the temperature rise test system for single battery

The size and nominal capacity of the single lithium battery used in the test are shown in Table 1. The incubator in the test system uses the 202-0A model of Zhejiang Shaoxing Yanfei Instrument Company, with a controllable temperature range of 10-300°C. The electronic load adopts the high-power electronic load of Olef Company, with a maximum power of 2000W, an adjustable voltage of up to 150V, and an adjustable current of up to 100A. Fig. 1 is a schematic diagram of the

test system. Fig.2 is the location of the monitoring point, and Fig.3 and Fig. 4 are the thermostat and electronic load, respectively.

Table 1.

Lithium iron phosphate battery parameters

Legend	Size/mm	Quality/kg	Voltage /V	Nominal capacity /Ah	Maximum charge discharge ratio
	180*130*30	1.395	Standard voltage 3.2 Stop voltage 2.5	50	1/5C

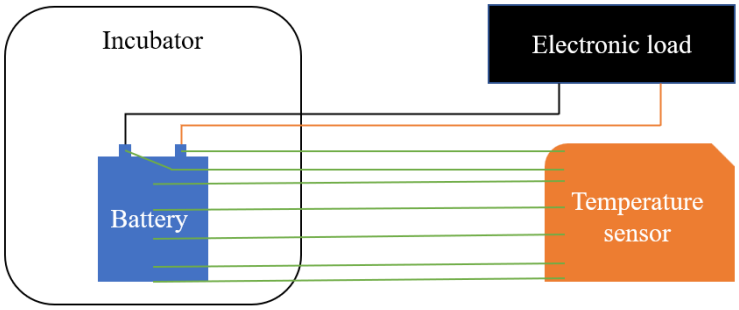

Fig. 1 Schematic diagram of the temperature rise test system

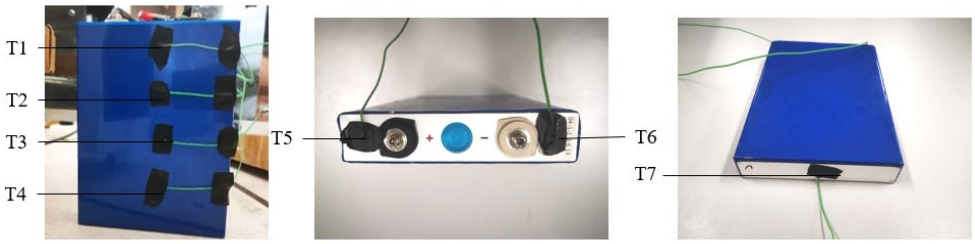

Fig. 2 Battery temperature monitoring points

Fig. 3 Incubator for test

Fig. 4 Electronic load for test

2.2 Analysis of test results

The temperature rise curves of 1C and 2C discharge rates of the single

prismatic lithium battery at 25°C are shown in Fig. 5 and Fig. 6, respectively. It can be seen from Fig. 5 that as the discharge time increases, the temperature of each monitoring point gradually rises. The highest temperature occurs at the T5 monitoring point (positive pole), and the highest temperature is 38.7°C. The temperatures of the seven monitoring points are arranged in descending order as T5>T6>T1>T2>T3>T4>T7, and the temperature gradually decreases from the top to the bottom of the battery. From the temperature rise curve of 2C discharge rate in Fig. 6, it can be seen that the temperature rise of the seven monitoring points is roughly the same as 1C. The highest temperature also appears at the T5 monitoring point, and the highest temperature is 47.6°C.

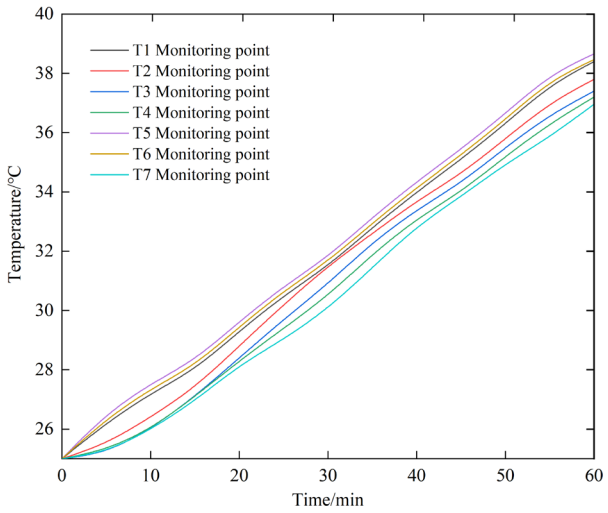

Fig. 5 Temperature rise curve of each monitoring point under 1C discharge rate

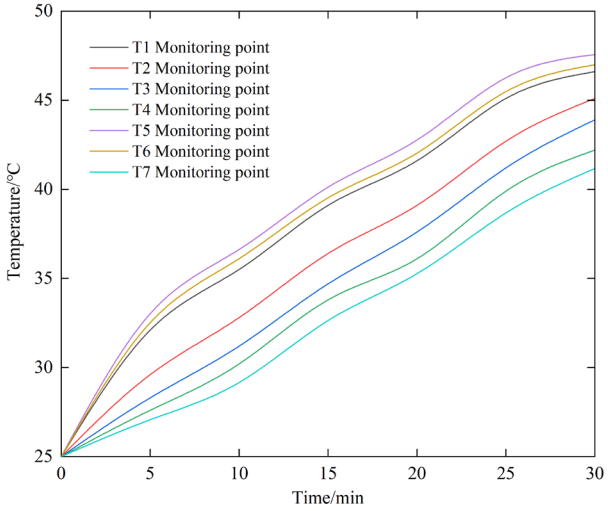

Fig. 6 Temperature rise curve of each monitoring point under 2C discharge rate

Fig. 7 shows the discharge temperature curve of a single battery at different rates. The temperature difference is obtained by calculating the temperature difference between T5 monitoring point (positive pole) and T7 monitoring point (battery bottom) of the battery in each time period. It can be seen from Fig. 7 that when the single battery is discharged at 1C, the temperature difference curve is relatively flat, with a temperature difference of about 1.5°C. When the single battery 2C discharges, the temperature gradient on the battery surface changes more obviously, and the average temperature difference in each time period is about 6.1 ℃. The imbalance of internal heat generation is enhanced, and the maximum temperature difference reaches 7.6 ℃, which is easy to cause local polarization of the cell and reduce the service life of the battery.

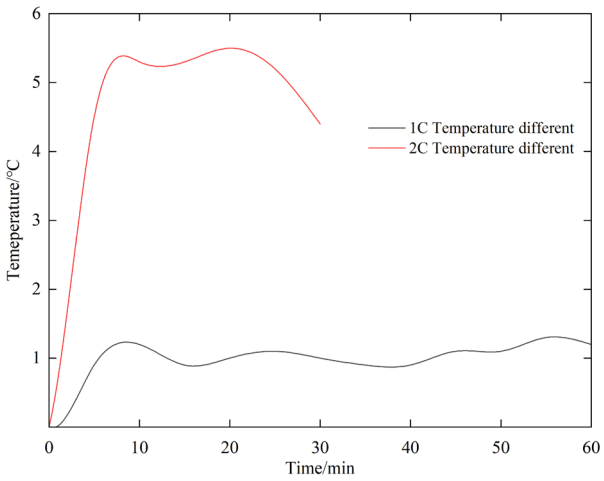

Fig.7 Temperature difference curve of single cell at different discharge rates

3. Construction of electrochemical thermal three-dimensional simulation model of single cell

3.1NTGP Table model

The NTG (Newman Tiedemann Gu) model was developed to mathematically model the constant current charge and discharge behavior of the battery [16]. When the NTG model is used, the difference between the simulated and measured battery temperature is less than 1°C [17]. The NTG model treats the battery as a voltage source (V) in series with a resistor (represented by the admittance term Y). The NTG model is shown in Fig. 8.

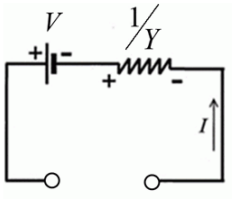

Fig.8 NTG model

The NTGP Table 3D model uses constant current density along the electrodes to predict the potential and temperature of the battery. The model takes into account the current changes along the height and width of electrode and the heating in the current collector. It also considers the capacity loss at a higher rate, that is, the Peukert effect, which can better improve the accuracy of the charging and discharging simulation of the battery. The control equation of the NTGP Table model is:

Operating Voltage:

$$V_{cell} = V(SOC_i, T) - \frac{i}{Y(SOC_i, T)} \tag{1}$$

Discharge:

$$SOC_i = 1 - (1 - SOC)\frac{C_{Ah-m-2,0}}{C_{Ah-m-2,i}} \tag{2}$$

Charge:

$$SOC_i = SOC\frac{C_{Ah-m-2,0}}{C_{Ah-m-2,i}} \tag{3}$$

$$SOC = \frac{\int idt}{C_{Ah-m-2,0}},\ i = \frac{I}{A} \tag{4}$$

Electrochemical heat generation:

$$Q = I \cdot \left(U_{oc} - V_{cell} - T\frac{dU}{dT}\right). \tag{5}$$

where, A is the electrode area; $C_{Ah-m} - 2{,}0$ is the nominal capacity; $C_{Ah-m} - 2, i$ is the capacity at current density i; i is the current density; Q is the electrochemical heat generation; U_{oc} is the balance voltage; V is the voltage terms; V_{cell} is the operating voltage, and Y is the admittance term.

3.2 Geometric model

A schematic diagram of the internal structure of a single lithium iron phosphate battery is shown in Fig. 9. The battery is composed of an anode plate, a diaphragm, a cathode plate, a collector end face, a bus bar and an outer shell. The geometric model and grid division of the single battery are shown in Fig. 10. A polyhedral grid is used for the single battery. Since the battery poles have a great impact on the overall heat generation, in order to improve the calculation accuracy, the positive and negative poles are grid-encrypted. The grid cells are 85466 and the grid faces are 541328. The simulation results of this paper have verified the grid independence.

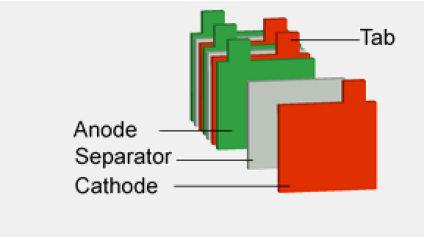

Fig. 9 Schematic diagram of single battery structure

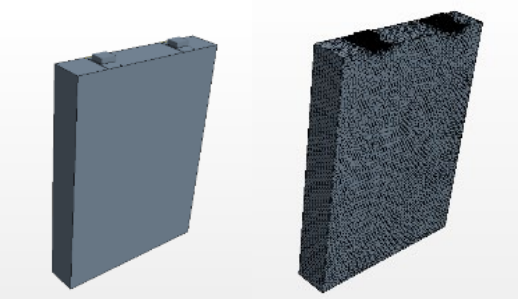

Fig. 10 Single cell geometry model and grid generation

3.3 Simulation parameter and boundary condition setting

The single cell is laminated, and its physical and chemical parameters are shown in Table 2. The positive and negative electrodes are set to LiFePO4 and graphite carbon rod, respectively. The reaction mode is lithium battery charge and discharge reaction. The discharge voltage is set to 3.2V, and the stop voltage is 2.5V. The thicknesses of the positive and negative electrode material coating are set to 0.08mm and 0.06mm, respectively. There is total 87 battery cells. After comprehensive settings, the battery capacity will reach 50Ah. The ambient temperature is to 298.15K (25°C). The heat dissipation coefficient of the battery surface simulates the condition of the incubator, which is 0W/mK. The battery shell is an aluminum shell, and the thermal conductivity is 217.7 W/mK. This article assumes that the positive electrode, negative electrode, separator layers, the core and shell are closely attached. The contact thermal resistance is ignored. The contact resistance caused by the welding of the inner tab and the outer pole is also ignored.

Table 2.

Physical and chemical parameters of lithium iron phosphate battery

Physicochemical parameters	positive electrode	negative electrode	Diaphragm	Positive collector	Negative collector
Materials	LiFePO4	Graphite	Polypropylene	Al Foil	Cu Foil
Thickness/ (mm)	0.160	0.120	0.150	0.020	0.010
Density/(g/cm3)	3.360	2.030	0.650	2.700	8.880

Porosity	0.096	0.240	65	——	——
Maclaurin number	——	——	8.500	——	——
Specific heat capacity / (J·kg-1·℃-1)	383	710	——	0.889	0.378
thermal conductivity / (W·m-1·℃-1)	1.0	1.0	——	235	400
Conductivity /(S/cm)	——	——	——	3550	5810

3.4 Model validation

Fig.11 is a cloud diagram of the temperature distribution of single cells with 1C and 2C discharge rates at an ambient temperature of 25°C. It can be seen that the high temperature of this battery is concentrated at the tab. The temperature at the positive tabs is the highest, which is consistent with the battery model simulation results of researchers such as PANCHAL [18]. The temperature distribution of this battery gradually decreases from the top to the bottom of the battery. The reason is that the internal material of the battery has a large electrical resistance and a small thermal conductivity, which makes it generate a lot of heat when discharging. At the same time, it cannot be effectively transferred, which ultimately leads to an uneven distribution of temperature on the physical scale. It can also be observed that under the same temperature condition, the higher the discharge rate, the greater the temperature rise of the cell.

Fig.12 is the temperature rise comparison curve of T1 monitoring point under 2C discharge rate. The simulation value of T1 monitoring point has roughly the same upward trend as the experimental value, and the maximum error is 1.04%. The built model can be used for further simulation research.

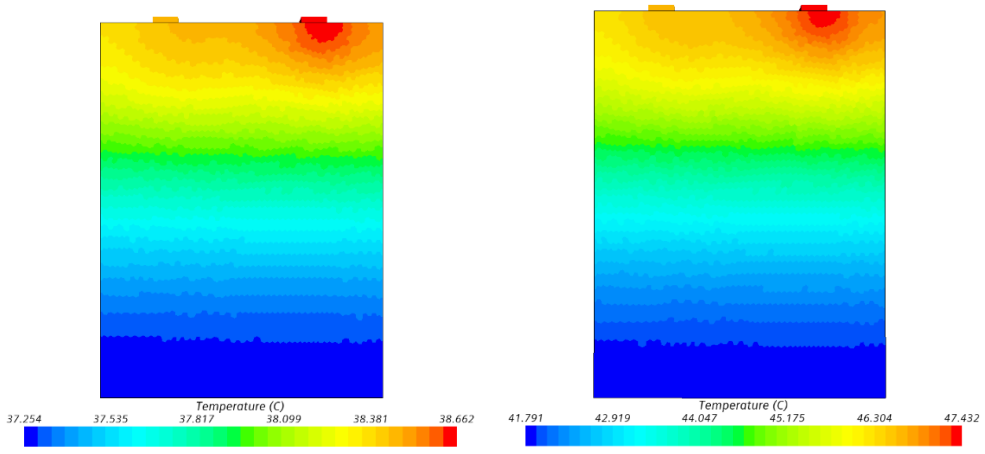

(a) 1C discharge cloud chart (b) 2C discharge cloud chart

Fig.11 discharge temperature cloud diagram of 1C and 2C at 25℃

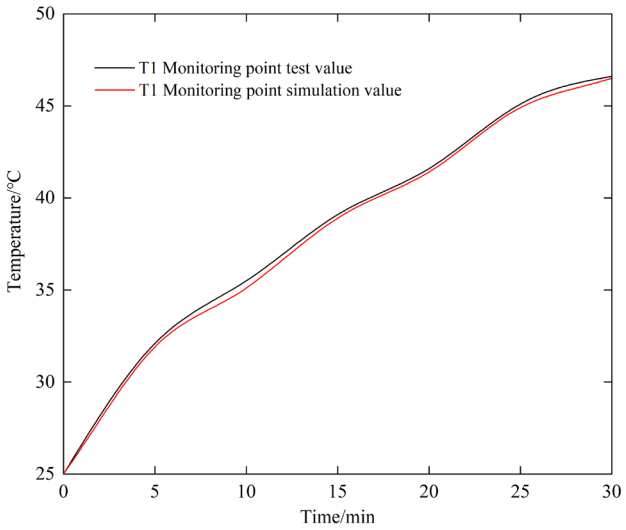

Fig. 12 Comparison curve of temperature rise at T1 monitoring point under 2C discharge rate

4. Simulation on the Temperature Rise Characteristics of Single Cell

4.1 The influence of current collector thickness on battery temperature distribution

Bipolar plate is the main conductive material of the battery, and its resistance is an important factor affecting the internal resistance. When the width of the bipolar plate is constant, the thickness of the collector becomes the main factor affecting the cross-sectional area of the material. In this paper, the current collector thicknesses of 12μm, 20μm, 30μm and 60μm are simulated and calculated, respectively. Fig. 13 shows the temperature distribution diagrams of the battery with different current collector thicknesses. It can be seen that the highest temperature of batteries with different current collector thicknesses all appear at the positive electrode tab. As the thickness of the current collector increases, the temperature of the negative electrode tab gradually becomes the second. Fig. 14 shows the temperature rise curves of batteries with different current collector thicknesses. It can be seen that the thickness of the current collector has a significant effect on the maximum temperature of the battery. The greater the thickness of the current collector, the lower the maximum temperature of the battery. The smaller the thickness of the current collector, the higher the battery temperature. This is because under the same material, the greater the thickness of the current collector, the smaller the resistance, the smaller the impact on the internal resistance of the battery, and the maximum temperature of the battery will also decrease.

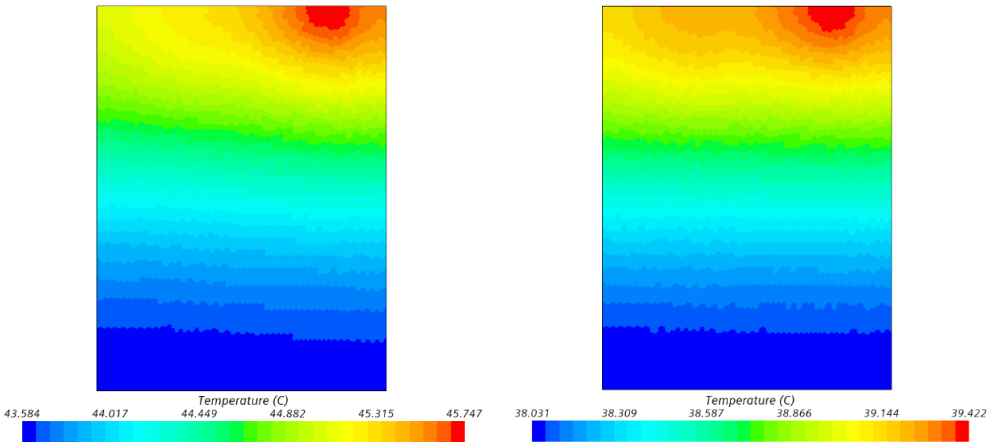

(a) 12μm (b)20μm

(c)30μm (d) 60μm

Fig.13 Battery temperature distribution with different current collector thicknesses

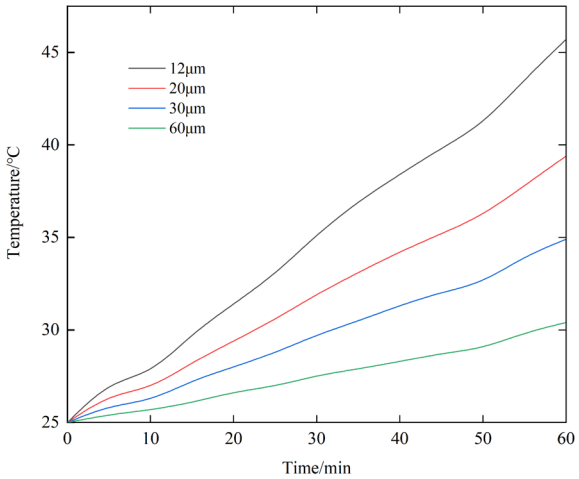

Fig.14 Temperature rise curves of batteries with different current collector thicknesses

4.2 The influence of current collector conductivity on battery temperature distribution

The conductivity of the current collector will also have a certain impact on the internal resistance of the battery. Fig. 15 is a battery temperature distribution diagram under different conductivity coefficients. The left is a front view of the battery, and the right is a cross-sectional view of the upper end of the battery. As shown in Fig.15, as the conductivity of the current collector increases, the highest temperature point of the battery gradually shifts from the positive tab to the negative tab. At the same time, from the temperature rise curves of batteries with different conductivity coefficients in Fig. 16, it can be seen that the higher the conductivity of the current collector, the lower the maximum temperature of the battery during discharge. The lower the conductivity of the current collector, the higher the maximum temperature of the battery. When the conductivity of the current collector increases, the influence on the maximum temperature of the battery during discharge is gradually reduced. The temperature difference between the conductivity of 1200S/cm and 3550S/cm is about 13.3℃, and that between the conductivity of 4800S/cm and 7600S/cm About 1.8°C.

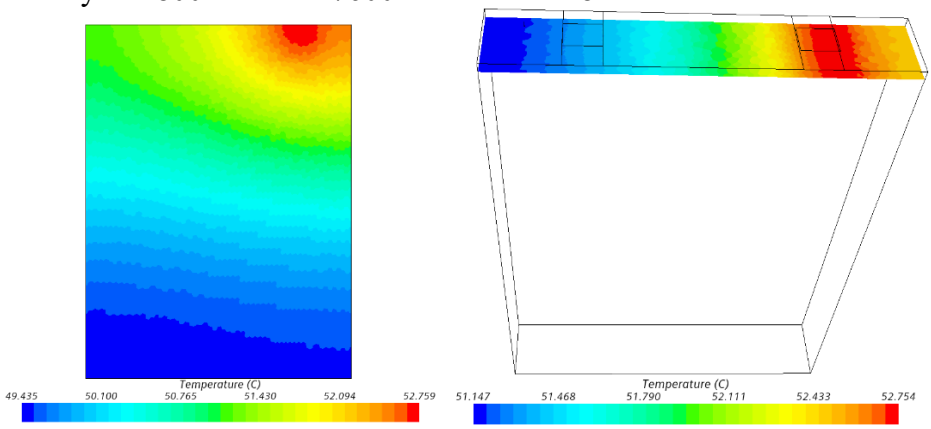

(a) 1200S/cm

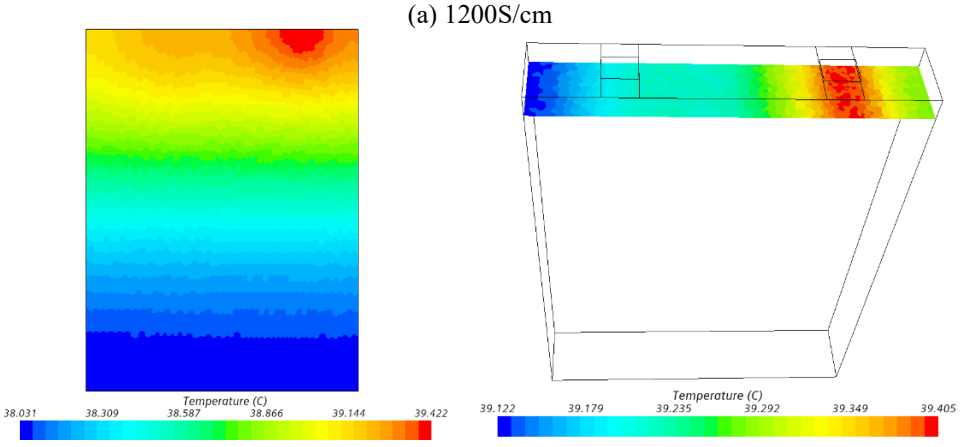

(b) 3550S/cm

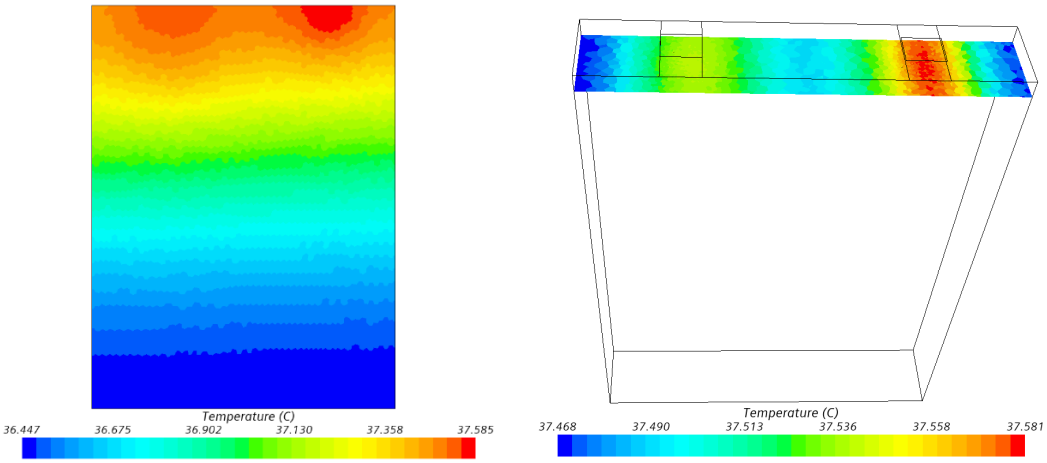

(c) 4800S/cm

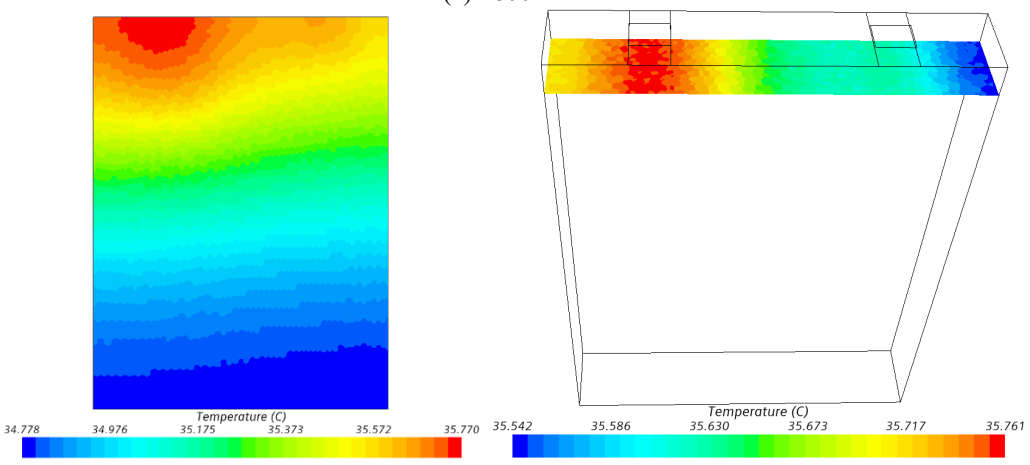

(d) 7600S/cm

Fig. 15 Temperature distribution and upper cross-sectional view of the battery with different conductivity coefficients

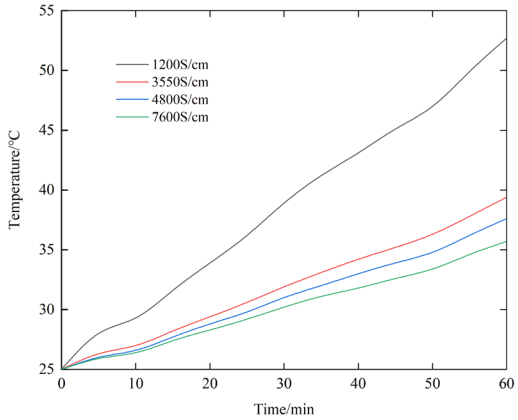

Fig. 16 Temperature rise curves of batteries with different conductivity coefficients

5. Conclusion and future work

In this paper, a temperature rise test system of single square lithium iron phosphate battery is built, and the temperature rise law curve and temperature field distribution of 1C and 2C rate discharge of lithium battery at room temperature are obtained. The NTGP Table model was used to construct the electrochemical-thermal coupling three-dimensional model of the single battery. The discharge temperature distribution and the maximum temperature under different current collector thickness and conductivity coefficients of the single battery are simulated. The results show that the electrochemical simulation of the battery using the NTGP Table model can describe the battery cell parameters in more detail, and the simulation results are more accurate. The temperature distribution of the single battery under different discharge rates is not uniform. The main trend is that the temperature gradually decreases from the positive and negative electrodes of the battery, and the highest temperature occurs near the positive tab, followed by the negative tab. The thickness and conductivity of the current collector have a significant impact on the temperature during discharge. The greater the thickness of the current collector, and the smaller the maximum temperature of the battery. The greater the conductivity coefficient, the lower the maximum temperature of the battery, and the maximum temperature difference under different conductivity coefficients reaches 17°C.

In this paper，according to the parameters and properties of the studied single cell, the battery design software is used to design the shape and size of the cell, the type of package and the parameters of the constituent materials (positive and negative collector, positive and negative mixed coating and diaphragm). In the future, the NGTP model can also be used for thermal simulation of other types of Li-ion batteries, such as cylindrical ternary Li-ion batteries, soft pack Li-ion batteries, and square LiCoO2 batteries

Acknowledgement

The work was supported by the Natural Science Foundation of Shandong (ZR2020MG017) and Philosophy and social science program of Qingdao (QDSKL2101167)

REFERENCES

[1] *Tete P.R, Gupta M.M, Joshi S.S.,* Developments in battery thermal management systems for electric vehicles: A technical review[J]. Journal of Energy Storage,2021,35: 102255.

[2] *Thomas S.B, Borislav D, George H, et al.,* Methodology to determine the heat capacity of lithium-ion cells. Journal of Power Sources, 2018, 395:369-378.

[3] *Choudhari V.G, Dhoble A.S, Satyam P*., Numerical analysis of different fin structures in phase change material module for battery thermal management system and its optimization[J]. International Journal of Heat and Mass Transfer,2020,163:120434.

[4] *Armando D.V, Arpit M, Matteo D, Massimo S, Massimiliana C.,* Transient thermal analysis of a lithium-ion battery pack comparing different cooling solutions for automotive applications[J]. Applied Energy,2017,206:101-112.
[5] *Karthik A, Kalita P, Garg A, Gao L, Chen SQ, Peng XB.* A Novel MOGA approach for power saving strategy and optimization of maximum temperature and maximum pressure for liquid cooling type battery thermal management system[J]. International Journal of Green Energy,2021,18(1).
[6] *Akbarzadeh M, Kalogiannis T, Jaguemont J, Jin L, Behi H, Karimi D, Beheshti H, Van M J, Berecibar M.* ,A comparative study between air cooling and liquid cooling thermal management systems for a high-energy lithium-ion battery module[J]. Applied Thermal Engineering,2021,198(2): 117503.
[7] *Zhang L.J, Li W.B, Cheng H.Z.,* Three-dimensional lithium-ion single-cell electrochemical-thermal coupling model. Power Technology, 2016, 40(07):1362-1366+1490.
[8] *LI J.J, Chen M.,* Modeling and simulation of electrochemical-thermal characteristics of lithium power batteries. Forest Engineering, 2020, 36(06):87-94.
[9] *Wang S.X, Zhang N, Gao M.* , Simulation Analysis of Thermal Management System of Lithium Battery for Power Vehicle. Thermal Science and Technology, 2016, 15(01):40-45.
[10] *Zhu F, He Y.Y, Chen Y.C, et al.,* Thermal design simulation study of bipolar lithium-ion batteries. Power Technology, 2021, 45(02):158-162.
[11] *Yang K, Shan Z.Q, Liu X.S, et al.*,Study on Thermal Simulation of LiNi0.5Mn1.5O4/Li4Ti5O12 Battery. Energy Technology, 2021, 9(5): 2000816.
[12] *Kuang K, Ren D.S, Han X.B, et al*. Simulation and analysis of the performance of large-size lithium-ion power batteries for vehicles. Journal of Automotive Safety and Energy, 2021, 12(01):116-124.
[13] *Sheng L, Xu H.F, Su L, et al*., Thermal characteristics and thermal physical properties of lithium ferrous phosphate batteries for automotive applications. Automotive Engineering, 2019, 41(10):1152-1157+1171.
[14] *Veth C, Dragicevic D, Merten C.,* Thermal characterizations of a large-format lithium-ion cell focused on high current discharges. Journal of Power Sources, 2014, 267(3):760-769.
[15] *Ye K.W, Xiang K.F, Li L.C.,* Simulation analysis and research on the thermal characteristics of VDA square power lithium battery. Power Technology, 2020, 44(04):514-517+581.
[16] *Shashank A, Weixiang S, Ajay K.,* Critical analysis of open circuit voltage and its effect on estimation of irreversible heat for Li-ion pouch cells. Journal of Power Sources,2017,350:117-126.
[17] *Celik A, Coban H, Gocmen S, et al.,* Passive thermal management of the lithium-ion battery unit for a solar racing car. International Journal of Energy Research, 2019, 43(8): 3681–3691.
[18] *Panchal S, Dincer I, Agelin-chaab M, et al.,* Transient electrochemical heat transfer modeling and experimental validation of a large sized LiFePO4/ graphite battery. International Journal of Heat and Mass Transfer, 2017, 109: 1239-1251.